



Investigation of changes in vegetation cover associated with changes in its hydro-climatic drivers in recent decades over North Sub-Saharan Africa

Faustin Katchele Ogou^{1,2} · Tertsea Igbawua^{2,3}

Received: 15 August 2021 / Accepted: 12 May 2022 / Published online: 30 May 2022
© The Author(s), under exclusive licence to Springer-Verlag GmbH Austria, part of Springer Nature 2022

Abstract

The environmental change in Northern Sub-Saharan Africa (NSSA) remains a challenge in relation with hydro-climatic variations and the low adaptation capacity of the region. The present study investigates the vegetation cover (NDVI) change associated with variations in hydro-climatic indicators over the period 1982–2015. The conventional statistical techniques such as the linear and multiple regressions, Mann–Kendall test, and the Pearson’s correlation were employed. The vegetation cover based on vegetation (NDVI) and hydro-climatic data were used. Trends in vegetation cover and hydro-climatic variables had monotonically increased except for the soil moisture that had monotonically decreased in the region. The proportion of significant positive (negative) changes was 46.78% (8.10%), 38.13% (0.34%), 52.12% (0.10%), 82.86% (0.00%), and 10.54% (38.27%) for NDVI, precipitation, potential evapotranspiration, temperature, and soil moisture, respectively. The low vegetation cover dominated the NSSA region with a proportion of about 32% of the total area coverage. The vegetation classes including low coverage, very high coverage, and extreme high coverage exhibited increasing trends. Meanwhile, moderate coverage and high coverage exhibited decreasing trends. The area-averaged precipitation and temperature were positively correlated with the NDVI; however, the area-averaged soil moisture showed negative association with NDVI. Spatial significant positive (negative) correlations of NDVI with the precipitation, temperature, and soil moisture at the 5% level occupied 1.67% (11.59%), 3.37% (26.19%), and 10.24% (6.75%), respectively. However, the combine effects of hydro-climatic variables are better for the monitoring of vegetation cover. This confirms that the vegetation cover is influenced by many factors such as soil moisture, temperature, and precipitation.

1 Introduction

Climate change is presented as a process that will in one way or another disturb living things and ecosystems all over the world (Cetin 2020a). The Sub-Saharan African is one of the regions exposed to the effects of climate change with a low adaptability capacity. As consequences of climate change, the environment monitoring and the food security

crisis remain challenges. Moreover, the region experiences the fastest growing rate of population (e.g., West Africa with 2–3% of growing rate that was reported by (Aklesso et al. 2018)). While some regions experience positive effect of climate, others undergo harsh conditions of it, which are not static with time. Most of previous studies time spanning is in general either shorter or different region from that of the present work. For example, Du et al. (2015) argued that it is important to better apprehend the NDVI changes and their climate drivers during longer time scales with the latest dataset because it constituted a limitation for climate-NDVI relationship study (Herrmann 2007). Among the regions negatively influenced by climate change/variability in the world, NSSA constitutes one of the hotspots of climate change (Müller et al. 2014). It was noted with a strong evidence that the precipitation is not only the climatic variables that contributed to the greening of Sahel region (Leroux et al. 2017); hence, the causes of greening of the Sahel region remain an opened debate due to the diverge of

✉ Tertsea Igbawua
tertsea.igbawua@uam.edu.ng

¹ Institute of Atmospheric Physics, CAS Key Laboratory of Regional Climate-Environment for Temperate East Asia, Chinese Academy of Sciences, Beijing 100029, China

² University of Chinese Academy of Sciences, Beijing 100049, China

³ Federal University of Agriculture, Benue State, Makurdi, Nigeria

researchers views on the vegetation dynamics (Hein et al. 2011). Furthermore, there is a limited plan and support for the environment monitoring. For instance, Schlenker and Lobell (2010), and Karlson and Ostwald (2016), showed that there is limited investment in scientific research to assess the impact of environmental changes by countries of the NSSA region, which is facing food security crisis.

Several studies have paid attention to the dynamical change of ecosystems nowadays (Bachelet et al. 2001; Traore et al. 2014; Xu et al. 2016a, b; Zhang et al. 2016; Pei et al. 2018). The climatological disasters notably, droughts, have caused many fatalities in the Eastern part of Africa with more than one-third of the population affected in Djibouti, Eritrea, and Somalia followed by West and South Africa (Lukamba 2010). Moreover, Knauer et al. (2014) mentioned that lives of millions of West African people were interrelated with vegetation dynamics. These events have affected undoubtedly the ecosystems of the area as well as the water resources (Vlek et al. 2008). NDVI has been one of the variables used widely to characterize the ecosystem and land cover at the annual and interannual time scales (Barbosa et al. 2006; Dardel et al. 2014; Pravalie et al. 2014). A particular interest exists in studying the impacts of climate change on agriculture in Sub-Saharan Africa, and on vital investments to support an adjustment to climate fluctuations (Schlenker and Lobell 2010). The interannual and intraseasonal variability of vegetation index revealed a robust photosynthetic activity over the Sahel, which was interrelated to above-normal convection and rainfall within the intertropical convergence zone (ITCZ) in the summertime (Philippon et al. 2007). It was also associated partly with colder (warmer) SST in the eastern tropical Pacific (the Mediterranean) (Philippon et al. 2007). Previous studies have investigated the relationship between climate factors and the normalized difference vegetation index (NDVI) and found that precipitation and soil moisture, temperature somehow played a role in the greening of Sahel (Zhang et al. 2005; Olsson et al. 2005; Bégué et al. 2011; Karlson and Ostwald 2016; Brandt et al. 2016; Igbawua et al. 2016; Zewdie et al. 2017; Leroux et al. 2017). However, the temporal coverage of the data available for these studies was short. For instance, over the Northern Sub-Saharan Africa (NSSA), the precipitation behaved differently regarding the length of studied period (Ogou et al. 2019), i.e., while observing increasing of precipitation over the period from 1990 to 2016, in contrast, it showed a decreasing trend over 1960–2016. Over approximately the NSSA, it was reported that between 1982 and 2006, the degree of correlation of all the meteorological variables (precipitation, air temperature, and specific humidity) with productivity varies according to locations; hence, no one formulation is appropriate for the whole region (Rishmawi et al. 2016). A long-time period of NDVI data would be more helpful to identify departures in primary production

for entire ecological zones, for instance, the Sahelian zone (Tucker 1986). A study has attributed the changes in the greenness observed over the sub-Saharan to climatic factor (e.g., rainfall) and non-climatic drivers (e.g., soil moisture) (Hoscilo et al. 2015). Over the Niger, a country of Sahel has developed a practice called as farmer managed natural regeneration and has contributed to the increasing trend in vegetation greenness (Haglund et al. 2011). The climate and non-climatic factors that contribute to the sub-Saharan greenness are not fully studied.

The classification of NDVI has been adopted by many authors for deepening the understanding of the vegetation cover changes (e.g., Al-doski et al. 2013; Nath and Acharjee 2013; Peng et al. 2019). According to Brown (2018), NDVI values vary from +1.0 to –1.0, and the areas of barren rock, sand, or snow usually indicate very low NDVI values (for example, 0.1 or less). The author added that sparse vegetation namely shrubs and grasslands or senescing crops may result in moderate NDVI values (approximately 0.2 to 0.5). Besides, high NDVI values (approximately 0.6 to 0.9) correspond to dense vegetation that is usually observed in temperate and tropical forests or crops at their peak growth stage (Brown 2018). Changes in climatic variables can lead to disasters such as floods, droughts, and landslides, in certain areas. For example, a study has demonstrated how disasters can affect the settlement of people in a district of Turkey, Atakum (Kilicoglu et al. 2021). In addition, the temperature and precipitation were found to be among the variables that contributed to biocomfort structure in Bursa (Cetin 2019). Meanwhile, the comfort based on climate was dependent on geographical conditions, which affected human daily activities, settlement, and living standards (Cetin 2020b). Climate variables were also successfully used in studying the tourism comfort in Imzir (Adiguzel et al. 2021).

Significant degradation of vegetation was linked to water deficit as a consequence of combined effects of decreased in precipitation and increased of potential evapotranspiration in Asia (Xu et al. 2016a, b). The vegetation cover has been also used to study the relationship between resource capital and fertility in countries of Sub-Saharan Africa (Nigeria, Cameroun, Senegal, and Burkina-Faso), which study showed a strong association but complex (Sasson and Weinreb 2017). The urban vegetation has been used to characterize urban vegetation based on the NDVI values in Malaysia (Hashim et al. 2019). A positive change in NDVI in Sahel has been observed since 2002 according to earlier studies (Eklundh and Olsson 2003), but the positive change proportion of NDVI was less than the demand in biomass of the area (Abdi et al. 2014). All the above-mentioned authors highlighted that many variables contribute to change in NDVI over the region; however, the precipitation and soil moisture were the main focus. For instance, an index such as Niño3.4,

the sea surface temperature index is the main mode of National Center for Environmental Prediction (NCEP) surface temperature variability in a window centered over Africa, and regional-scale indices based on NCEP surface temperatures and atmospheric variables (relative humidity, geopotential heights, and winds) (Martiny et al. 2010). A dominant positive correlation coefficient was obtained between total water storage anomaly and NDVI in NSSA for the period from 2002 to 2015 (Ogou et al. 2021). However, such in-depth analysis using the combination of multiple hydro-climatic variables had not been studied yet in NSSA.

To our knowledge, the classification of vegetation based on NDVI values has not yet been studied over the area, which is important to comprehend the vegetation dynamics. Therefore, this is the first study that classifies vegetation cover based on NDVI values over the northern Sub-Saharan Africa (NSSA). Moreover, the relationship of these classes with hydro-climatic factors still uncovered. Furthermore, quantitative study of changes in these variables was not shown in recent decades. Therefore, in regard to the above-mentioned information, the objectives of the study are as follows: classify the vegetation cover based on the NDVI threshold values to understand which classes undergo decrease or increase tendency and their drivers; analyze the relationship between vegetation cover of the region and the hydro-climatic drivers; investigate the tendencies in vegetation cover and hydro-climatic variables. The results of the analysis will be important for land cover and land use management, monitoring of the hydro-climatic variables over the region.

2 Data and methods

2.1 Study area

In order to give a sub-regional analysis of the climate and NDVI parameters, the NSSA region was divided as eastern Sahel (ES) (eastern Ethiopia), northern Sahel (NS), and the Guinea Coast (GC) and presented in Fig. 1. The ES was seriously affected by recurrent, erratic rainfall and high and increasing of temperature conditions (Mulugeta et al. 2017). They also showed the seasonality of rainfall over the region, which was from June to August. Wagner and da Silva (1994) argued that the rainfall regime in the NS was also featured by a boreal summer rainy season, but this season was shorter. The study reported that the NS rainfall was highly correlated with a pattern of positive SST anomalies in the North Atlantic and negative SST anomalies in the South Atlantic implying a positive meridional gradient near the Equator. The GC was the region receiving more rainfall compared with others regions. A positive relationship is found between the precipitation of this region and the southern oscillation Atlantic Ocean (Okoro et al. 2017). The period of more rainfall is from June to September (Wagner and da Silva 1994).

2.2 Data

The high-resolution data of the world's meteorological stations over land areas are obtained from the climatic research unit (CRU) of the University of East Anglia (Harris et al. 2014). The monthly precipitation (PRE), temperature (TMP)

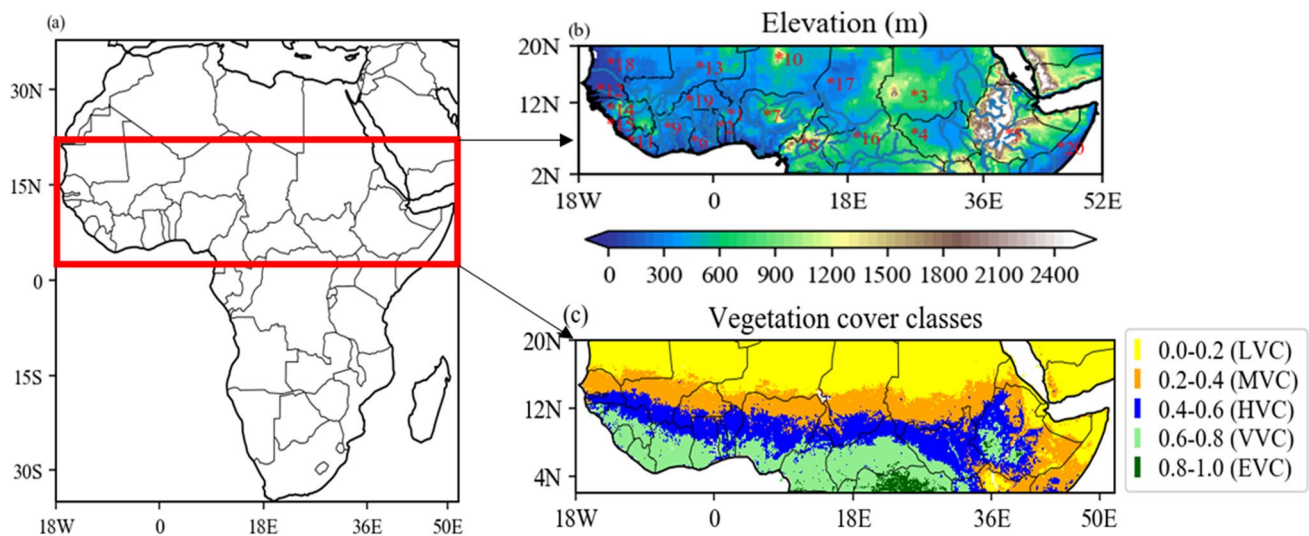


Fig. 1 Map of **a** Africa showing the study area in red rectangle, **b** the elevation, and **c** the classification of vegetation cover based on NDVI values. The asterisk (*) with numbers in red represent countries (1 = Benin, 2 = Togo, 3 = Sudan, 4 = South-Sudan, 5 = Ethiopia,

6 = Ghana, 7 = Nigeria, 8 = Cameroun, 9 = Ivory Coast, 10 = Niger, 11 = Liberia, 12 = Senegal, 13 = Mali, 14 = Guinea, 15 = Sierra-Leone, 16 = Central African Republic, 17 = Chad, 18 = Mauritania, 19 = Burkina-Faso, and 20 = Eritrea)

and potential evapotranspiration (PET) with a spatial resolution of $0.5^\circ \times 0.5^\circ$ (lon/lat) are used. The temporal coverage of the CRU datasets is from 1901 to 2016, and they are freely available at the following link: https://crudata.uea.ac.uk/cru/data/hrg/cru_ts_4.01/cruts.1709081022.v4.01/.

The climate prediction center (CPC) soil moisture data of a single column of depth 160 mm provided by NCEP Reanalysis data provided by the NOAA/OAR/ESRL PSD, Boulder, CO, USA, from their web site at <https://www.esrl.noaa.gov/psd/> (Dool 2003) was used. The temporal coverage of the data was from 1948 to near present at the spatial resolution of $0.5^\circ \times 0.5^\circ$. It has been successfully used in NSSA to investigate the relationship between NDVI and soil moisture (Ahmed et al. 2017).

Likewise, we collected the normalized difference vegetation index (NDVI) data sets from <https://ecocast.arc.nasa.gov/data/pub/gimms/3g.v1/>, which has a horizontal resolution of $1/12^\circ \times 1/12^\circ$ and a temporal spanning from July 1981 to 2015 (Pinzon and Tucker 2014). The dataset was generated from the advanced very high-resolution radiometers (AVHRR) global inventory modeling and mapping studies (GIMMS) third generation (NDVI) using an artificial neural network derived model. These datasets are preferred because it is recommended 30-year period for a climatological study (Table 1). The GIMMS-NDVI is used because of it has the longest time spanning, which more suitable for climate analysis and as proxy for vegetation greenness (Herrmann et al. 2005).

2.3 Methods

The GIMMS improvement scheme through the empirical mode decomposition (EMD) transformation method (Pinzon et al. 2005) implied that the GIMMS NDVI dataset is dynamic by nature and must be recalculated every time that more recent data are added (Fensholt and Proud 2012). At the global scale, the MODIS NDVI showed a good relationship with NDVI3g (Fensholt and Proud 2012). Hence, the NDVI3g (NDVI) is used through this work. The increase in NDVI has been interpreted as vegetation recovery from the Sahel drought (Herrmann et al. 2005; Olsson et al. 2005).

The original NDVI resolution has been up scaled to $0.5^\circ \times 0.5^\circ$ using the arithmetic means of six by six windows to match the resolution of hydro-climatic datasets (Zhang et al. 2017). The NDVI calculation is expressed as the difference between red (RED) and near-infrared (NIR) reflectance with the following formula: $NDVI = \frac{NIR-RED}{NIR+RED}$. The non-vegetation cover area (i.e., $NDVI \leq 0$) was masked out before the analysis. The distribution characterizing the NDVI values in the NSSA was give. NDVI's classes were defined as follows: 0.0–0.2, 0.2–0.4, 0.4–0.6, 0.6–0.8, and 0.8–1.0 for low vegetation coverage (LVC), moderate vegetation coverage (MVC), high vegetation coverage (HVC), very high vegetation coverage (VVC), and extreme high vegetation (EVC), respectively. Similar classification has been adopted by researchers to understand the dynamics of the vegetation cover (Peng et al. 2019; Yang et al. 2019). A study over western Africa showed that fires had a profound influence on the composition of the present forest canopy (Swaine 1992). This classification will help for in-depth analysis of effect of climate drivers on vegetation cover.

The term correlation used in statistics described a linear statistical relationship between two random variables. Therefore, the relationships between the variations of climate factors of sub-regions were assessed over the period 1982–2015 for NDVI, PRE, PET, TMP, and SM. Before investigating the drivers of NDVI change, we conducted the test of collinearity between the climate factors using the variance inflation factor (VIF) and matrix correlation (r). The stronger the relationship is, the stronger the correlation is. The given formula is as follows:

$$r = \frac{\sum_{i=1}^n (X_i - \bar{X})(Y_i - \bar{Y})}{\sqrt{\sum_{i=1}^n (X_i - \bar{X})^2 * \sum_{i=1}^n (Y_i - \bar{Y})^2}} \quad (1)$$

where X_i is the annual value of each variable, \bar{X} (\bar{Y}) is the mean value of a variable in all years, Y_i is the annual of a climate factor (e.g., TMP, PRE, SM) in all years, n is the number of samples; r is the correlation coefficient between

Table 1 Summary of data used in the study

Data sources	Variables	Spatial resolution	Time-frame	Time resolution	Missing values in NSSA (%)
CRU.ts4.01	PRE	$0.5^\circ \times 0.5^\circ$	1901–2016	Monthly	14.1
CRU.ts4.01	TMP	$0.5^\circ \times 0.5^\circ$	1901–2016	Monthly	14.1
CRU.ts4.01	PET	$0.5^\circ \times 0.5^\circ$	1901–2016	Monthly	14.4
CPC	SM	$0.5^\circ \times 0.5^\circ$	1948–2019	Monthly	13.8
AVHRR-GIMMS	NDVI3g	$0.083^\circ \times 0.083^\circ$	1981–2015	Bi-weekly	15.6

NB: The percentage of missing values showing here are mostly the water areas such as rivers, lakes and Atlantic Ocean coast in white color over NSSA

X_i and Y_i . The r is useful because it provides the degree of agreement between two variables.

The departures have been used to describe the regional climatic at global (Jones and Hulme 1996), continental (Nicholson 1980, 2000), and regional (Nicholson and Kim 1997) scales. It should be mentioned that the missing values of each parameter were ignored in the calculation (they were ignored because most variables did not have values over the ocean) processes.

$$\text{Std.Ano.} = \frac{X_i - \bar{X}}{\sigma} \quad (2)$$

where X_i is the yearly dataset, \bar{X} is the time-mean of the whole area of the variable. Negative A indicates a decrease of variable, and positive A indicates an increase in it. The equation is defined as:

$$\bar{X} = \frac{\sum_{i=1}^n X_i}{n} \quad (3)$$

where n is the total number of data.

The linear regression and non-parametric trends tests were used to show the tendency in hydro-climatic variables and the NDVI. The MK test was also applied to verify whether the tendency showed by linear trend is monotonic. The linear regression is expressed as follows:

$$Y_i = b_0 + bX_i + \varepsilon \quad (4)$$

where b_0 represents the constant (when $b=0$), ε the residual error, and b the regression coefficient. The regression coefficient equation is given:

$$b = \frac{n \times \sum_{i=1}^n X_i Y_i - \sum_{i=1}^n X_i \sum_{i=1}^n Y_i}{n \sum_{i=1}^n X_i^2 - (\sum_{i=1}^n X_i)^2} \quad (5)$$

Moreover, the multiple regression based on the ordinary least square (OLS) was used. The following equation represents the multi-regression model:

$$\frac{\text{NDVI}_i - \overline{\text{NDVI}}}{\sigma_{\text{NDVI}}} = \beta_1 \frac{\text{PRE}_i - \overline{\text{PRE}}}{\sigma_{\text{PRE}}} + \beta_2 \frac{\text{TMP}_i - \overline{\text{TMP}}}{\sigma_{\text{TMP}}} + \beta_3 \frac{\text{SM}_i - \overline{\text{SM}}}{\sigma_{\text{SM}}} + \varepsilon \quad (6)$$

where over-bar represents the mean over the whole area, $\beta_1, \beta_2, \beta_3$ represent the slope, σ is the standard deviation, and ε is the residual error of each variable. Furthermore, each variable was standardized to circumvent the problem of the units.

The Mann–Kendall (MK) test (Gilbert 1987; Kendall 1975; Mann 1945) was applied to assess statistically the possible existence of a monotonic upward/downward tendency of the drought indicators. We applied the sequential MK technique to emphasize the abrupt change. The following formula is given for the MK trend analysis:

$$S = \sum_{i=1}^{n-1} \sum_{j=i+1}^n \text{sign}(x_j - x_i) \quad (7)$$

where S is the statistical trend and,

$$\text{sign}(x) = \begin{cases} +1 & \text{if } (x_j - x_i) > 0 \\ 0 & \text{if } (x_j - x_i) = 0 \\ -1 & \text{if } (x_j - x_i) < 0 \end{cases} \quad (8)$$

where n is the length of the time series data set and $x_i \dots x_j$ stand for the observations at times i to j , correspondingly. According to the hypothesis of independent and randomly distributed random variables, the S statistic is approximately normally distributed when $n \geq 8$, as follows:

$$E(S) = 0 \quad (9)$$

$$V(S) = \frac{n(n-1)(2n+5) - \sum_{i=1}^j t_i(t_i-1)(2t_i+5)}{18} \quad (10)$$

where j is the number of tied groups and t_i is the size of the i th tied group. As a result, the standardized Z (calculated in the case of MK) test statistics follow a normal standardized distribution:

$$Z = \begin{cases} \frac{S-1}{\sqrt{V(S)}} & \text{if } S > 0 \\ 0 & \text{if } S = 0 \\ \frac{S+1}{\sqrt{V(S)}} & \text{if } S < 0 \end{cases} \quad (11)$$

A significance test is determined based on the result of the Z value. The sign of Z either positive or negative is indicating an upward or downward trend of the tested variable. Based on the outputs of the Z value, the trend is not rejected when the Z value is greater in absolute value than the critical value $Z\alpha$, at a selected significance level of α . The evaluation of correlation between regions is important for facilitating the prediction and monitoring of sub-regions' climate conditions given that of the other (Yim et al. 2014). To classify the NDVI values, we have used the mask function of numpy package in python 3. Pearson correlation and regression analyses were employed to examine the linkage between the sub-regions through the defined variables, the vegetation cover change drivers and the tendencies are investigated using the regression and MK trends tests. The present study focuses on period between 1981 and 2016 for the hydro-climatic variables and 1982 and 2015 for NDVI. Hence, relationships between NDVI and hydroclimatic drivers are analyzed over the time interval between 1982 and 2015.

3 Results

3.1 NDVI variation and its proportion

Figure 2 showed the monthly climatology of the NDVI in NSSA from 1982 to 2015. The NDVI decreased slightly from January to February where it reached its minimum (NDVI value about 0.28). Nevertheless, from March to September, the vegetation has increased whereby peaking in September and gradually decreased from October to December. The peak of the NDVI recorded in September was 0.41. The lowest NDVI value recorded in December is 0.31.

Figure 3 depicted the area percentage of each vegetation coverage class of annual NDVI. The classes of annual NDVI such as the LVC, MVC, HVC, VVC, and EVC occupied 32.02%, 18.37%, 17.08%, 14.77%, and 1.22%, respectively (See Fig. S1 for the spatial distribution).

3.2 Temporal trends in annual climate variables, annual NDVI, and the relationships between the sub-regions

Figure 4 showed the trends in hydroclimatic variables and the area covered by each class of vegetation as shown in Fig. S2. It can be seen that most regions experienced greening trends as depicted by the NDVI analysis (Fig. 4a). The slope change rate in NDVI was 0.0005 year^{-1} , 0.0009 year^{-1} , 0.0001 year^{-1} and over the NSSA, GC, and NS respectively, which were significant at the 5% level ($p < 0.05$).

Figure 4b showed that trends in NSSA, GC, NS were significant and positive during the period of the study. Slope change rates in PRE were $0.22 \text{ mm year}^{-1}$, $0.30 \text{ mm year}^{-1}$, and $0.15 \text{ mm year}^{-1}$ for the regions such as NSSA, GC, and NS, respectively. At this time, the trend in PRE over the ES

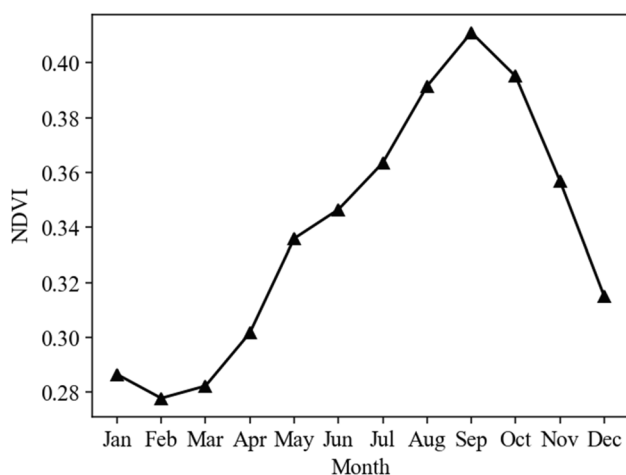


Fig. 2 Monthly Climatology of NDVI for the period 1982–2015

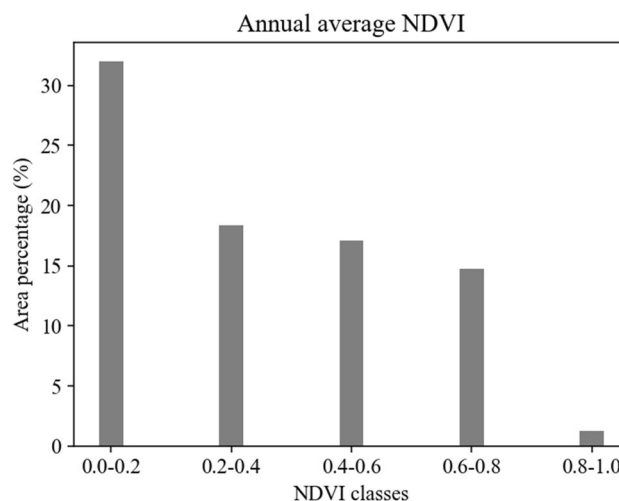


Fig. 3 Histogram of the area percentage of classes in NDVI for the period between 1982 and 2015

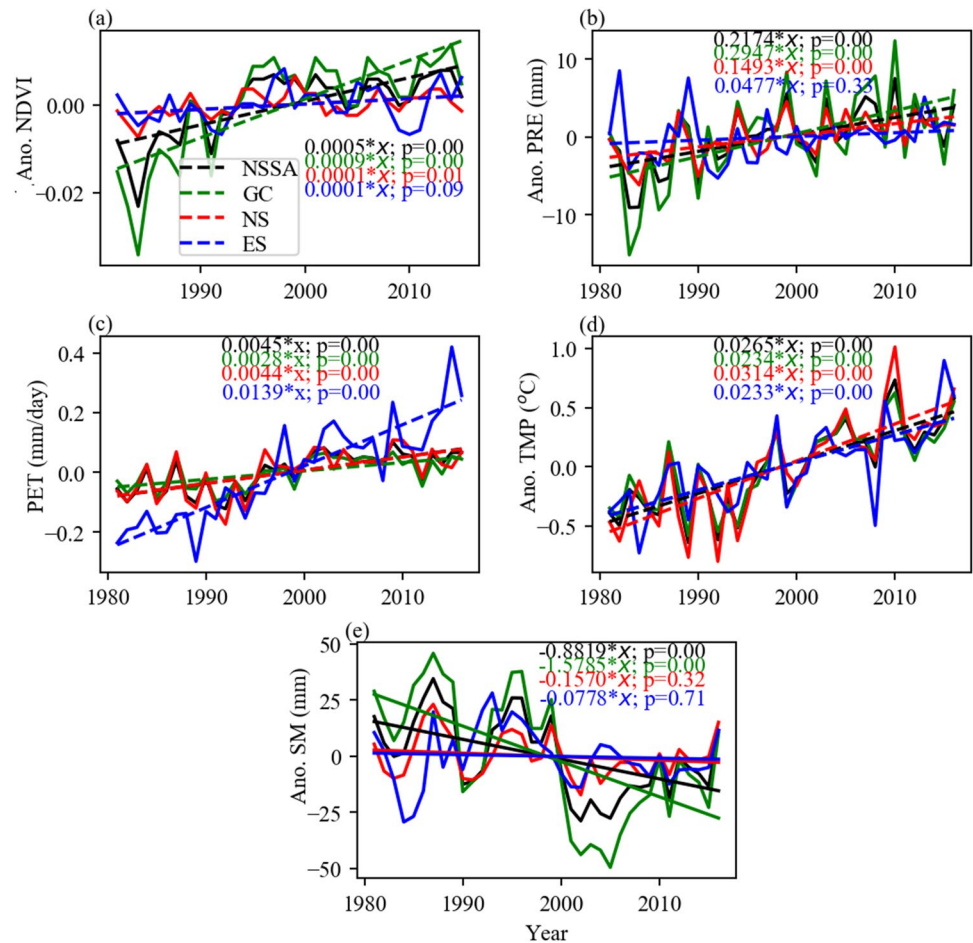
was positive, but with a non-significant change rate. The change rate of PRE over the area (ES) was $0.05 \text{ mm year}^{-1}$.

Significant positive variation rates in PET were obtained over the NSSA (Fig. 4c). Indeed, slope change values of $0.45 \text{ mm day}^{-1} \text{ year}^{-1}$, $0.28 \text{ mm day}^{-1} \text{ year}^{-1}$, $0.44 \text{ mm day}^{-1} \text{ year}^{-1}$, and $1.39 \text{ mm day}^{-1} \text{ year}^{-1}$ in PET were acquired in the NSSA, GC, NS, and ES, respectively; which were significant at the 5% level. It can be seen that the ES experienced the highest change rate in PET, while the GC experienced the lowest in it.

Figure 4d displayed the slope change rate in TMP over a 34-year period. A significant positive change rate in TMP was evident with the values of $0.0265 \text{ }^\circ\text{C year}^{-1}$, $0.0234 \text{ }^\circ\text{C year}^{-1}$, $0.0314 \text{ }^\circ\text{C year}^{-1}$, and $0.0233 \text{ }^\circ\text{C year}^{-1}$ for the NSSA, GC, NS, and ES, respectively. The region NS undergone the warmest rate in comparison with other regions (NSSA, GC, and ES). The ES experienced the least increasing change rate in temperature for the period of the study.

In Fig. 4e, SM exhibited downward tendencies in each of the four regions. Significant slope change values of $-0.8819 \text{ mm year}^{-1}$, $-1.5785 \text{ mm year}^{-1}$ over NSSA and GC were obtained in SM, respectively whereas insignificant slope change values of $-0.1570 \text{ mm year}^{-1}$ and $-0.0778 \text{ mm year}^{-1}$ over NS and ES were revealed, respectively. In general, a decrease in SM was evident during the study period in this region. The highest change rate in SM was observed over GC, while the lowest change rate was observed in ES. The tendencies in hydro-climatic variables and NDVI detected by the linear regression trend test were significant at the 5% level and were monotonic (Table S1). Although the SM showed a decline tendency over the 36 years (1981–2016), it could be noted over the GC region that between 1981 and 2005, the SM decreased

Fig. 4 Temporal variations and its linear trends in **a** NDVI (1982–2015), **b** PRE, **c** PET, **d** TMP, and **e** SM (1981–2016) over the NSSA



followed by an increase from 2006 to 2016. A similar tendency is observed for the NSSA region.

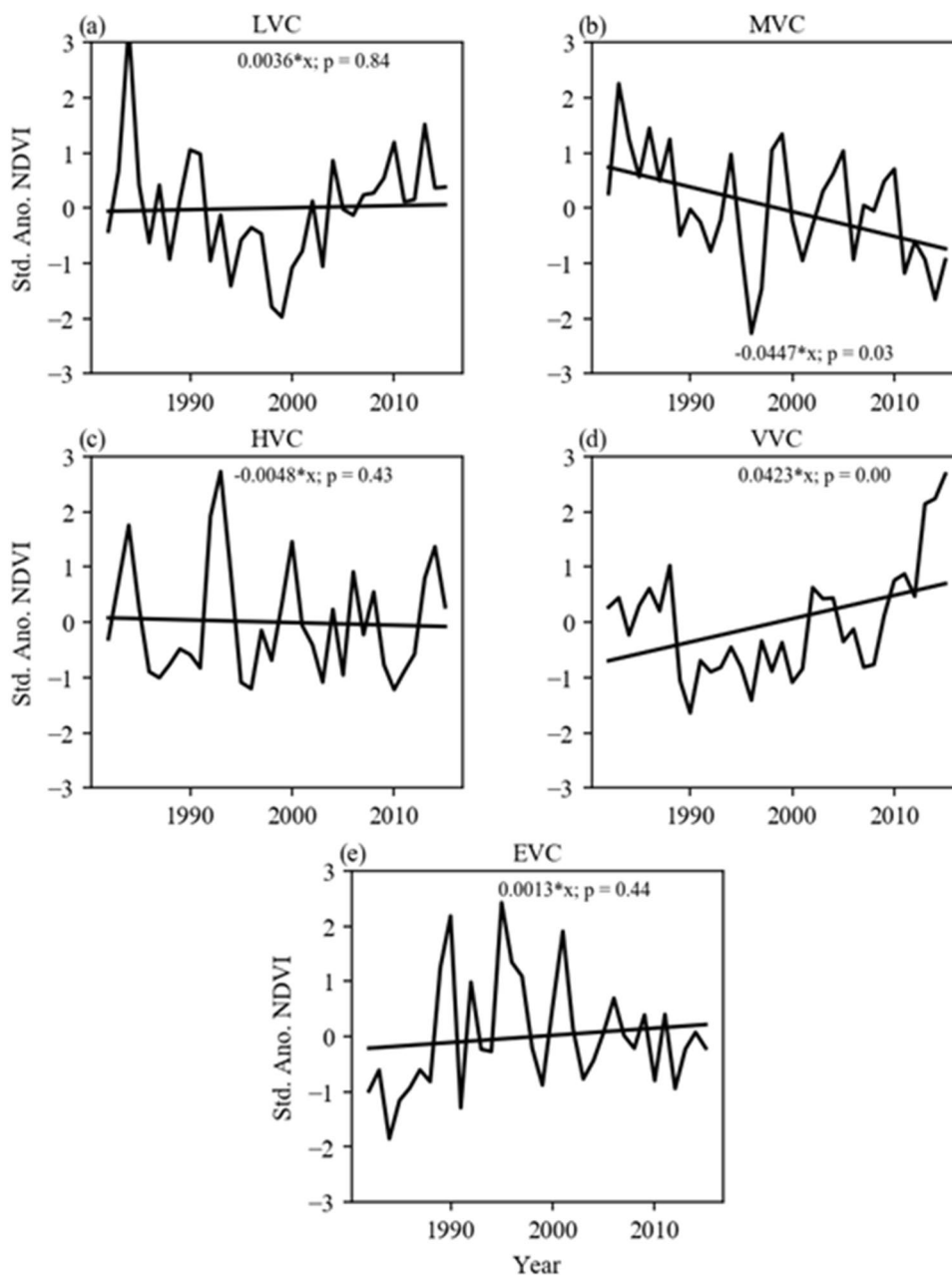
The technique would show the confidence of the analysis over NSSA and its sub-regions (NS, GC, and ES), i.e., the confidence of association between climate variables of the sub-regions. The NDVI of NS correlated with the NDVI of ES, but was found to be insignificant at the 5% level ($r=0.31$, $p=0.08$), whereas the NDVI of remaining regions were significantly correlated with one another over the same period. It was found that PRE of ES and that of the NSSA were not significantly interrelated at the 5% level. The association coefficient of these two regions was significant at the 15% level ($r=0.25$ and $p=0.14$). Non-significant correlations of the GC with the ES and that of NS with ES based on PRE at the 5% level were palpable. The association coefficients were 0.21 ($p=0.22$) and 0.14 ($p=0.42$), respectively. The SM of GC correlated with the NDVI of ES was insignificant at the 5% level with a correlation coefficient $r=0.28$ and $p=0.09$; in contrast to remaining regions where significant relationships were observed based on this variable. At this time, the associations of the variables such as PET and TMP over the GC with that of the ES, GC with

NS, NS with ES, NSSA with GC, NSSA with NS, and NSSA with ES were significant at 5% level.

3.3 Temporal trends in annual NDVI classes

The linear trend in the time series of the vegetation class was depicted in Fig. 5. The LVC and HVC showed a weak upward and downward tendency with a value of 0.0036 ($p=0.84$) and lowest anomaly of LVC was obtained in 1999. Two important variation periods could be observed such as declining tendency between 1982 and 1999, which is followed by an increasing tendency from 1999 to 2015. It can be noted that a continuous declining in MVC with the lowest anomaly observed in 1996 over the region of study. It meant that the low vegetation cover slowly ameliorated over time while the moderate vegetation of the NSSA reduced slowly over the region. Variations in vegetation cover classes such HVC, VVC, and EVC did not exhibit distinct years of low (high) anomalous values. Figure 5b showed a decreasing trend in MVC with the change rate of -0.0447 ($p=0.03$) that was significant ($p<0.05$), which translated into reduction in moderate vegetation cover. In Fig. 5d, an upward tendency could be seen in VVC with a change rate of 0.0423

Fig. 5 Variations in NDVI classes with its linear trends over the NSSA



($p=0.00$) that was statistically significant ($p < 0.05$). That implied that very high vegetation cover had increased. A positive upward tendency was gotten from an EVC (Fig. 5e) with a non-significant change rate with a slope of 0.0013 ($p=0.44$). The extreme vegetation cover had been weakly ameliorated over the region in the past 34 years.

3.4 Spatial distribution based on MK and linear trends of annual hydro-climatic and NDVI

The results of the MK trends (Fig. 6) patterns are analyzed in this section due to its similarity with that of linear trends (Fig. S3). Dominant positive changes of the NDVI could

be observed over the NSSA (Fig. 6a). However, some locations showed adverse changes in NDVI, for example, part of eastern Mauritania, western Mali, southwestern and central eastern of Niger, eastern of Sudan and central Ethiopia. A significant change at a 5% level was evident over considerable parts of the area. The maximum and minimum slope change rates of NDVI for the whole region were 0.81 and -0.78 , respectively. Positive trends in NDVI occupied a proportion of 64.46%, whereas negative trends accounted for 19.40% of the total area. Among the proportion of positive (negative) trends in NDVI, 30.85% (3.91%) were significant at the 5% level, respectively.

Fig. 6 Distribution of the MK trend for **a** NDVI, **b** PRE, **c** PET, **d** TMP, and **e** SM over 1982–2015. The dots indicate significance at the 5% level

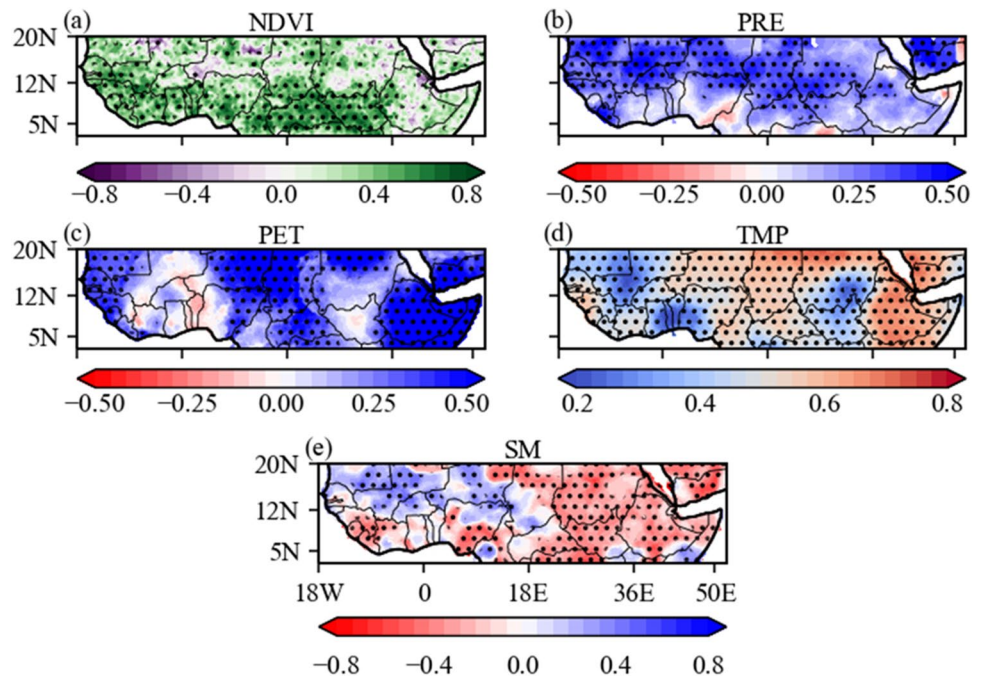


Figure 6b exhibited positive and negative changes in PRE during the period of study. Large areas of the NSSA experienced a positive change in PRE, whereas small areas of the region experienced a negative change in it. We observed a negative change in PRE over southeastern Nigeria, northwestern Cameroon, and parts of Eritrea. The maximum and minimum slope change rate in PRE of the whole region was 0.56 and -0.44 , respectively. The positive trend in PRE occupied a proportion of 78.15%, whereas 6.88% presented negative trends over the total area. Among the proportion of positive (negative) trends in PRE, 18.23% (0.14%) was significant, correspondingly.

The PET showed a significant positive trend (at the 5% level) over a considerable part of the area (Fig. 6c). Meanwhile, a small part of the area exhibited significant negative trends, presented for the regions of South Sudan, southwestern Niger, Mali, northernmost of Burkina-Faso, Ivory Coast, Ghana, and eastern Guinea. The maximum and minimum slope change rates of the PET of the whole region were 0.78 and -0.26 , respectively. The positive trend in PET occupied a proportion of 76.41%, whereas a proportion of 9.17% revealed the negative trend in the total area. Among the proportion of positive (negative) trends in PET, 35.67% (0.00%) was significant, correspondingly.

Figure 6d displayed the trend in TMP in NSSA. It could be seen that significant positive trends were dominated in the region. That meant that TMP had increased over the NSSA area over the last 34 years. The warming trend observed in TMP could be due to the increases in CO_2 . However, the very weak decreasing tendency of TMP was observed over southeastern Sudan, Benin, Togo, eastern Ghana, western

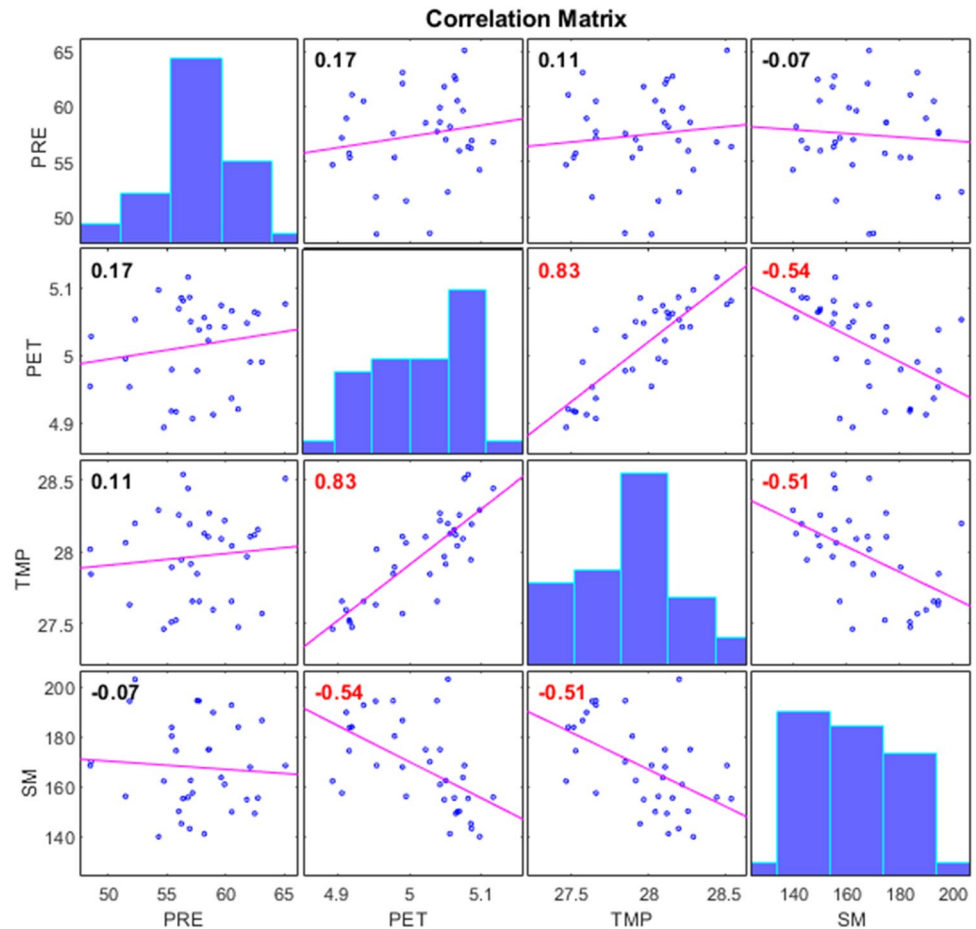
Nigeria, and a noteworthy part of Mali. The lowest proportion of trends in TMP was 0.02%, whereas that of the highest was 85.93% of the total area. The maximum and minimum change rates in TMP were 0.16 and 0.75, respectively. Among the proportion of positive (negative) trends in TMP, 75.99% (0.00%) was significant.

Heterogeneous trend patterns were observed in SM (Fig. 6e); it showed that the regions within the NSSA experienced varying conditions (increasing or decreasing) of soil moisture. The proportion of negative trends in SM was 60.02%, whereas that of positive trends in SM was 26.23% of the total area. The maximum and minimum change rates in SM were 0.6 and -1.00 , respectively. Among the proportion of positive (negative) trends in SM, 3.57% (20.12%) was significant, respectively. The region located between 12°N to 20°N of latitude and 18°W to 18°E of longitude is dominated by a positive variation in SM.

3.5 Matrix correlation and collinearity via variance inflation fraction tests of hydro-climatic drivers

The correlation matrix is used to evaluate the association between hydro-climatic factors as shown in Fig. 7. To check the multicollinearity between the climate drivers, the matrix correlation and the variance inflation fraction (VIF) tests are used. A significant correlation ($r=0.83$) is found between PET and TMP, it means that when the temperature increases, the potential evapotranspiration increases. Significant negative correlations of SM with PET and TMP are obtained, i.e., when temperature increases, the soil moisture decreases through the increase of potential evapotranspiration.

Fig. 7 Matrix Correlation between hydro-climatic factors. Units: PRE (mm), PET (mm day⁻¹), TMP (°C), and SM (mm). The values in red indicate significance at the 5% level



The VIF test shows that TMP and PET have high values (greater than 3), respectively. The combination of the correlation coefficient and that of VIF indicated a slight collinearity between variable TMP and PET. The VIF test for the variables PRE, TMP, and SM is repeated and it showed low values (less or equal to 1.4). Hence, the variable PET is eliminated in the afterwards of the study for enhancement of the consistency of relationships between hydro-climatic drivers and NDVI.

3.6 Relationships between single hydro-climatic factors and NDVI classes

The relationship between hydroclimatic factors and annual average NDVI and the time series of each NDVI class is assessed based on the Eq. (4).

The association of the climate factors (PRE, TMP, and SM) with each class of the NDVI (LVC, MVC, HVC, VVC, and EVC) was examined (Table 3) during 1982–2015. We have approximated the hydro-climatic factor time series of the area corresponding with each NDVI class. A positive correlation between PRE and EVC was obtained, which was not significant at the 5% level. However, negative

associations of PRE with LVC, MVC, HVC, and VVC were obtained, respectively. Among these NDVI classes, the LVC was the sole class that was highly linked to the precipitation anomaly. The increase of precipitation was associated with a significant decrease in LVC but with a weak decreasing trend in moderate, high, and very high vegetation cover during the study period. The very high ecosystem class increased when precipitation increased. The growth of the EVC class was somehow dependent on the precipitation. Meanwhile, the precipitation played a reduced role for LVC, low, moderate, and high vegetation cover.

A non-significant negative correlation between TMP and EVC was obtained. The negative connection of TMP with EVC suggested that a decrease in TMP followed by an increase in EVC. The rise in temperature was not beneficial for very high vegetation in NSSA. However, a positive association of TMP with LVC, MVC, HVC, and VVC during 1982–2015 was obtained. This signified that influences of TMP on LVC, MVC, and HVC ecosystem classes were weak though positive. Besides, the interaction of TMP with VVC was significant. The growth of high vegetation was influenced by the rising of temperature.

The vegetation coverage such as the LVC, MVC, and EVC classes was negatively linked to SM. The negative linkage coefficient meant that an increase in SM led to a decrease in low, moderate, and extreme vegetation cover. Elevated soil moisture reduced the development of these vegetation classes. Nevertheless, the ecosystem classes such as HVC and VVC were weakly and positively associated with SM. Values indicated a positive relationship of SM with HVC and VVC. That meant that an increase in SM is related to a weak increase in moderate and high vegetation categories.

3.7 Relationships between single hydro-climatic variables and NDVI

On one hand, the connections between area average time series of NDVI and precipitation while temperature and soil moisture are assessed on the one hand (Fig. 8) through a simple regression. The slope change rate of the NDVI during anomalous PRE, TMP, and SM is $0.0014 \text{ mm year}^{-1}$, $0.0098 \text{ }^{\circ}\text{C year}^{-1}$, and $-0.0001 \text{ mm year}^{-1}$, respectively. Statistically significant linear relationship at the 5% level is found between NDVI and PRE and TMP time series. Thus, the area average precipitation and temperature are indicators of positive change in area average NDVI.

On the second hand, point-to-point correlation were examined and presented in Fig. 9. Positive and negative

correlations coefficient between NDVI and PRE, TMP, and SM are found. The areas that experienced positive (negative) correlation between PRE and NDVI occupied 23.73% (48.83%). Significant positive (negative) at the 5% level of these correlations occupied 1.67% (11.59%). Positive (negative) correlations of NDVI with TMP occupied 15.22% (57.60%) of the total area, while significant positive (negative) correlations at the 5% level exhibited 3.37% (26.19%) of it. The area that experienced positive (negative) correlation between SM and NDVI occupied 42.91% (41.04%). Significant positive (negative) correlations at the 5% level occupied 10.24% (6.75%). Somehow, the precipitation, temperature, and soil moisture contributed differently to the variation of NDVI.

3.8 Multiple regression of hydro-climatic divers on NDVI

The combination of the climate drivers such as area-averaged PRE, TMP, and SM showed significant relationship with area-averaged NDVI over the 34-year period ($r=0.491$, $p<0.01$). However, the SM plays a negative role while the PRE and TMP play positive influence on NDVI. A non-significant slope change rate of $-0.0900 \text{ year}^{-1}$ ($p>0.6$) is obtained between soil moisture and NDVI. Concerning the precipitation and NDVI, a significant slope change rate of 0.5819 year^{-1} ($p<0.01$) was acquired while NDVI

Fig. 8 Scatter plots of area-averaged NDVI with **a** PRE, **b** TMP, and **c** SM for the period from 1982 to 2015. The points represent area-averaged values of each parameter

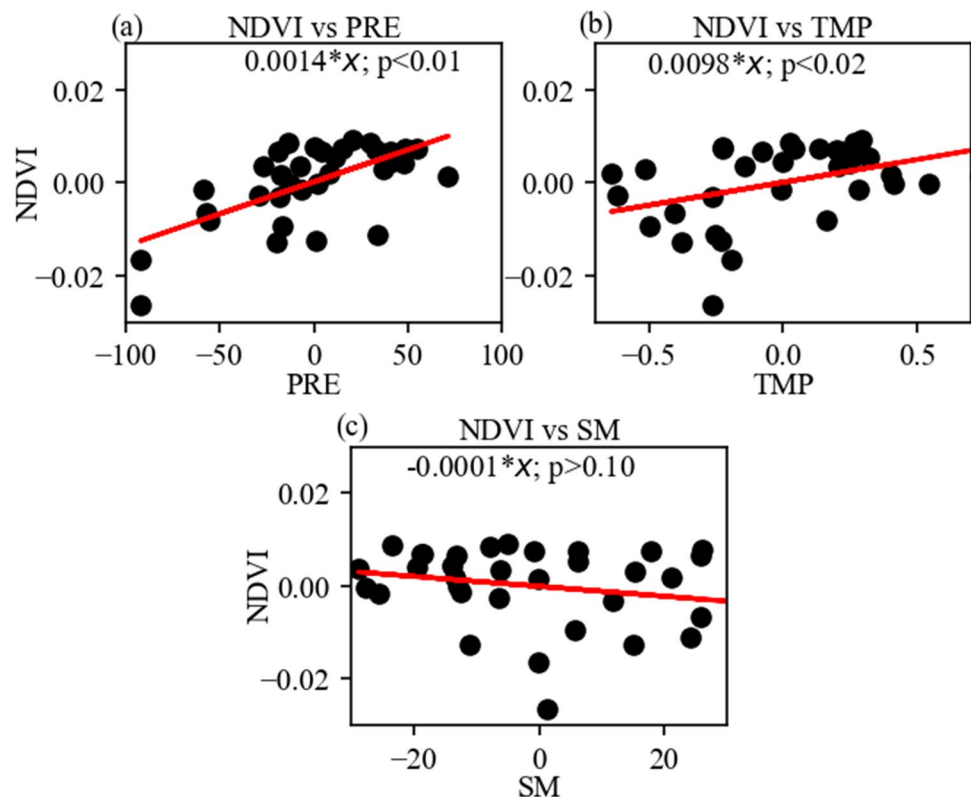
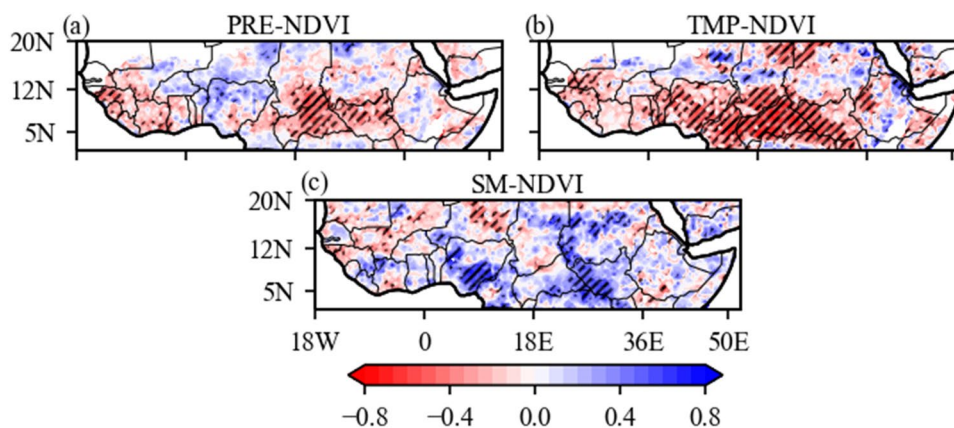


Fig. 9 Spatial distribution of correlations coefficients of NDVI with **a** PRE, **b** TMP, and **c** SM for the period from 1982 to 2015. The hatches represent significant at the 5% level



responded favorably to positive change in temperature with a significant slope change rate of 0.4274 year^{-1} ($p < 0.10$), respectively. We also, considered removing TMP to comprehend whether PRE and SM are sufficient enough to assess the relationship between NDVI and climate drivers. The result showed that the combination of the PRE, TMP, and SM parameters are better than considering two parameters (PRE and TMP). For illustration, the regression based on a single driver of NDVI change has been analyzed. Positive change in NDVI corresponded with positive change in precipitation with a correlation coefficient $r = 0.5849$ and $p < 0.01$. Similarly, the temperature responded positively with positive change in NDVI with a correlation coefficient $r = 0.3542$ and $p < 0.01$. Meanwhile, the soil moisture responded negatively to positive variation in NDVI.

3.9 Multiple regression of hydro-climatic drivers on NDVI classes

The hydro-climate drivers showed a significant association with LVC. The precipitation ($r = -0.1648$, $p = 0.274$) and soil moisture ($r = -0.4055$, $p = 0.023$) are negatively correlated with the LVC, whereas it is positively correlated with the temperature ($r = 0.0848$, $p > 0.10$). When the precipitation and soil moisture increase, the low vegetation cover decreases. The predicted NDVI and original NDVI showed significant relationship with $r = 0.47$ and $p = 0.005$. However, when suppressing the temperature, the confidence level of association between the predicted and original NDVI was reduced; this means that the combination of climate factors is preferred to predicting the low vegetation cover than using a single variable.

The hydro-climatic drivers ($r = 0.041$, $p = 0.738$) are non-significantly associated with the MVC. Indeed, the precipitation is weakly and negatively associated with MVC with an association coefficient $r = -0.1090$ and $p = 0.574$. Similarly, the temperature is weakly and negatively correlated with

MVC ($r = -0.1388$, $p = 0.530$). However, the soil moisture is weakly and positively associated with MVC with a correlation coefficient $r = 0.0219$ and $p = 0.912$. The increase of soil moisture resulted in increase of the medium vegetation cover. This means that the soil moisture is a limiting factor for the medium vegetation cover.

The HVC showed a significant relation with climate factors with an $r = 0.225$ and $p = 0.0508$). Meanwhile, the precipitation is negatively correlated with HVC with a correlation coefficient $r = -0.1648$ and $p = 0.274$, which is not statistically significant at the 5% level. The soil moisture is also negatively correlated with HVC with a correlation coefficient $r = -0.4055$ and $p = 0.023$ that is significant, whereas the temperature is positively correlated with HVC with a correlation coefficient $r = 0.0848$ and $p = 0.638$ that is not statistically significant.

Hydro-climatic drivers are not significantly associated with VVC in view of the $r = 0.159$ with $p = 0.151$. A non-significant but positive relationship is observed between VVC and TMP and SM. At this time, the TMP is significantly correlated with VVC ($r = 0.4482$, $p = 0.053$) at the 5% level, suggesting that temperature was an indicator of very high vegetation cover. However, the PRE is negatively connected with VVC, which is not statistically significant. It means that an increase of the precipitation is associated with a decreasing of the very high vegetation cover.

EVC is negatively associated with SM with $r = -0.2275$ and $p = 0.316$. Similarly, the TMP is found to be negatively interrelated with EVC with $r = -0.0558$ and $p = 0.815$. Meanwhile, the PRE is positively associated with EVC with a very correlation coefficient $r = 0.0037$ and $p = 0.984$. Overall, the EVC is not significantly related with these hydro-climatic drivers because $r = 0.040$ and $p = 0.741$. The extreme high vegetation cover increases when soil moisture and temperature decrease whereas an increase in it is associated with increase in precipitation. A continuous increasing in temperature as result of climate change is disastrous for certain categories of plants.

4 Discussions

The paper analyzed the recent change in hydro-climatic variables (1981–2016) and vegetation cover (1982–2015) over the NSSA using the Mann–Kendall test, simple linear regression and multiple regression analyses. It assesses the relationship of the hydro-climatic variables with the variations in the vegetation cover using the NDVI as proxy data. The examination of the variation in NDVI was indispensable to comprehend the vegetation role in regional and global ecosystem stability (Gu et al. 2018). To the extent of our knowledge, the temperature and the potential evapotranspiration received less attention in existing literature over the NSSA particularly in views of their relationship with NDVI. However, due to the collinearity of temperature with PET, the PET has been eliminated for the assessment of the NDVI drivers. The TMP considered in the current analysis had not been previously taken into account, though studies had emphasized the probably warming of the region as the result of climate change.

4.1 Hydroclimatic and NDVI trends

The two months (i.e., January and February) corresponded to the Harmattan (dry air) period and are dominated by the burning activities (bush fire). Therefore, high evapotranspiration due to high temperature and low precipitation induced the soil moisture-laden. These conditions could cause the low vegetation observed from January to February, in particular, the lowest value observed in February. The pattern of monthly NDVI dynamics obtained in our study was similar to that gotten in a previous study over the Guinea Coast (Aklesso et al. 2018), however, with different amplitude. The difference in amplitude could be investigated from spatial and temporal extents. According to Zhang et al. (2018), the weak value of NDVI in February was attributed to the decline in deciduous vegetation over the region of study. This reason could also be valuable for the NSSA region that was characterized by deciduous vegetation. From this result, the NSSA was dominated by sparse vegetation coverage, which is in line with Los (2013) who found that the sparse vegetation dominated over the Sub-Saharan Africa.

Approximately, for the NS area, a study by Kaspersen et al. (2011) has found a change rate of 0.0011 year^{-1} , which was not statistically significant. However, in the ES, the slope change rate in NDVI was 0.0001 year^{-1} that was non-significant at the 5% level. The positive slope change rate meant the entire NSSA had experienced increased vegetation cover. Dardel et al. (2014) found that trends in NDVI were positive everywhere in Sahel over 1982–2011, which is in agreement with our findings. The findings from the study indicated that the area-averaged NDVI at regional and

sub-regional scales over the period of study significantly increased. The increase of NDVI found is in agreement with previous studies over the Sahel region (e.g., Hänke et al. 2016). However, previous work did not pay attention to the categories of NDVI that contributed to the greening of Sahel despite browning of vegetation cover could be observed over parts of the NSSA. A study demonstrated that over Niger and Mali, some locations experienced negative change in vegetation, whereas others experienced positive change in vegetation (Dardel et al. 2014). According to the present analysis, the greening of NSSA would be attributed to positive change in the low vegetation cover, very high vegetation cover, and extreme high vegetation cover. Meanwhile, the medium vegetation cover, high vegetation cover undergone a declining tendency. Many factors such as soil water condition, modification of soil properties (Nicholson and Farrar 1994) or human activities (Spiekermann et al. 2015) or natural condition as well as the precipitation variability could explain negative trends in these classes. In contrast, Peng et al. (2019) found significant increasing trend in vegetation cover, which had a coverage index higher than 0.8 in comparison with the trend in the extreme high vegetation cover.

The spatial distribution of trend in NDVI showed a heterogeneous changes. The reverse change observed at spatial scale could be explained by the medium and high vegetation cover.

The NSSA experienced increases in PRE, TMP, and PET, but dominated by a declining trend in SM. The positive change in the precipitation time series of NSSA indicated that the precipitation had increased over the area during the period of study. The increase obtained for PRE and TMP are consistent with many studies conducted over the region (Collins 2011; Ogou et al. 2019). The atmospheric circulations contributed to the increase in PRE (Sindikubwabo et al. 2018). The positive change in PET implied that it had increased over the 1982–2015 time interval in the NSSA region. It is worth noting that the PET and TMP had increased over most parts of the area, however, received less attention by researchers compare with PRE and SM in relation with vegetation cover. The positive change in temperature signified that the entire NSSA was warming. Among the subdivisions, NS was the warmest area, while ES was the least warm area. The consistent increase of temperature could be attributed to elevated CO_2 emissions. Meanwhile, the SM decrease over most parts of the region. The decrease in SM could be explained by the high potential evapotranspiration under the effect of increase in temperature, which lead to a probable increase in precipitation. Besides the rising temperature effect, the decreasing trend observed in soil moisture over central Asia have been also linked to rising in radiation that could produce negative ecological impacts (Li et al. 2015).

4.2 Relationship of NDVI with single hydro-climatic drivers

The assessment of the relationship between the vegetation cover (NDVI) and each of hydro-climatic variables showed that the area-averaged NDVI is positive and significantly correlated with the area-averaged PRE and TMP, implying that regionally, they played (i.e., PRE and TMP) important roles in the growth of vegetation cover. The negative association of soil moisture with NDVI implied that when area average time series of soil moisture increased, the area average time series of NDVI decreased. However, point-to-point correlations between NDVI and hydro-climatic variables depicted a dominant positive association between NDVI and SM. This showed that the soil moisture rather plays a control factor, which is in line a previous work over the NSSA within period from 1982 to 2013 and found that the soil moisture was strongly connected NDVI (Ahmed et al. 2017). The dominance of the relationship soil-vegetation cover implied that areas experiencing increases in vegetation cover are associated with areas experiencing increases in soil moisture and decreases trends in vegetation cover is followed by decreases trends in soil moisture. This could explain the dominance of areas with positive correlation coefficient between soil moisture and vegetation cover over the region of study. Moreover, the result from correlation between the areas average time series, i.e., vegetation cover and soil moisture, could be different from that of point-to-point analysis because of discrepancies between the values of each point. The negative correlation obtained between PRE and NDVI over parts of NSSA region could be explained by the influence of human activities. For example, human activities such as expansions of agricultural areas and urbanization would have contributed negatively to the change in NDVI, although the precipitation had increased. A previous study over the Sahelian region of Burkina-Faso had also found a significant negative correlation coefficient between annual precipitation and land cover change, which was attributed to human activities (Lambin and Ehrlich 1997). It could also be explained by a decreasing in water use efficiency of certain categories of plants. It means that some plants are water tolerant while others non-water tolerant. The results of the area-averaged could be different from that of point-to-point analyses because of the values at a particular site (grid-point) could be minimized or maximized (influenced) by that of other sites. For example, it was mentioned that NDVI-rainfall connection is highly variable and depends on the degree of aggregation of those variables in the time and space domains (Wang et al. 2003). Results suggested that the conclusion from area-averaged correlations could not explain that of point-to-point correlations between variables, which is also powerful to characterize a region instead of specific locations.

4.3 Factors influencing vegetation cover and its classes

The multiple regression between hydro-climatic driver's effect on NDVI showed that area-averaged soil moisture is negatively associated with positive vegetation cover changes, but the area-averaged PRE and TMP are significantly and positively associated with positive change in vegetation cover. Results from multiple regression confirmed that of correlation assessment between area-averaged soil moisture, temperature and precipitation, and vegetation cover. Based on temporal relationship (area-averaged), it is found that PRE and TMP are contributing factors to the increasing trend of NDVI over the region of NSSA. Positive correlations found between area-averaged NDVI and precipitation and temperature are in agreement with Xu et al. (2014), who also found positive correlations of annual NDVI with annual precipitation and annual temperature. In-depth analysis was then carried out to comprehend the effect of hydro-climatic drivers on vegetation cover classes.

The multiple regression analysis between vegetation cover classes and hydro-climatic factors showed that the temperature was likely to control the low vegetation cover and high vegetation cover, while the soil moisture controlled the growth of the medium vegetation cover. This could be explained by the fact that these vegetation cover categories are sensitive to a high-amount of water. The positive association of low vegetation cover with temperature means that increase in temperature will lead to increase in evaporation hence reduce the soil water content. Meanwhile, the precipitation controlled the high vegetation cover and altogether precipitation, soil moisture, and temperature controlled very high vegetation cover with stronger relation with the temperature. The different reactions of the vegetation cover (NDVI) to the soil moisture could be due the depth at which the water is available for roots of each category of plants. Although the use of NDVI from GIMMS is important for analyzing vegetation cover over a longer period, there is limitation in using NDVI to identify the types of vegetation as the level of land cover data. Moreover, there are many other NDVI datasets (e.g., MODIS) that have higher resolution compare with that of GIMMS. Ahmed et al. (2017) showed that the data processing technique during the analysis could lead to different results, which is in agreement with different results obtained from different methods used in the present study, for instance, the point-to-point correlation (important for local decision) is different from that of correlation between area-averaged NDVI and SM (important the NSSA region) and different results when applying the multiple regression method beside the simple regression. It is worth noting that the simultaneous effect of three hydro-climatic factors is likely to be more useful for monitoring and predicting of vegetation cover over the NSSA. These findings are

important for environmental monitoring and policy making for the land cover both at regional and local scales.

5 Conclusion

This study is carried out to analyze changes in hydroclimatic variables and their interaction with changes in vegetation cover in the region where climate change is considered to be threatening the environment and, in particular, food security. The vegetation cover through the use of NDVI and hydro-climatic variables were analyzed for the period 1982–2015 over northern Sub-Saharan Africa (NSSA). The trends in hydro-climatic variables and NDVI were studied. NDVI classes and trends were also computed, and the relation between the NDVI classes and hydro-climatic variables was examined. The trend analysis showed that precipitation, temperature and potential evapotranspiration, and NDVI had increased during 1982–2015, but the soil moisture has decreased. The NSSA has been divided into three sub-regions within which the trends and Pearson correlation in hydro-climatic variables were applied. The entire sub-regions showed an increasing trend of hydro-climatic variables and NDVI. Meanwhile, it is found that temporal evolution of PRE, PET, and TMP can be predicted knowing the tendency in each of the three sub-regions for the time interval of study over the NSSA region.

The classification of the vegetation cover using NDVI showed that the region is dominated by the low vegetation with approximately an area coverage of 37%. Types of vegetation cover had increased mainly the low, very high, and extreme vegetation's covers (i.e., LVC, VVC, and EVC, respectively) when others including high and medium vegetation covers (i.e., MVC and HVC, respectively) had decreased over the 34-year period. The Pearson correlation test revealed a complex relationship with vegetation cover classes. On other hand, the multiple regression analysis showed a different correlation coefficient of vegetation cover classes with the combined hydro-climatic drivers.

The temporal relationship showed a significant association of the NDVI with precipitation and temperature. The temperature was revealed an important factor as well for the vegetation cover change over the NSSA, which may be resulted from the global warming effect. Meanwhile, the spatial distribution depicted the SM as the factor contributing to the greening of the region. The potential evapotranspiration is collinear with precipitation based on matrix and variance inflation fraction tests. The multiple regression showed that spatially, the soil moisture is the most contributor to the greening of NSSA, though the contribution from the temperature and precipitation were also significant, which is consistent with previous studies showing that not only the precipitation or soil moisture drove the greening over NSSA

in recent decades. More studies are needed to comprehend better about the greening of this region especially using field data, which is necessary for its environmental monitoring and food security. It is also important for forestry and watershed managements.

Supplementary Information The online version contains supplementary material available at <https://doi.org/10.1007/s00704-022-04088-3>.

Acknowledgements We sincerely thank CAS-TWAS and the UCAS for their support during our Ph.D. program. We also appreciate the World Meteorological Organization (WMO) for their support, which allowed us to study in this field. We also thank the anonymous reviewers for their insightful and helpful comments to improve the present work.

Author contribution Conceptualization: Faustin Katchele Ogou; methodology: Faustin Katchele Ogou; data analysis and draft: Faustin Katchele Ogou and Tertsea Igbawua; original manuscript draft: Faustin Katchele Ogou; supervision and review: Tertsea Igbawua.

Data availability All the data used in the work are available in the public domain and can be freely downloaded at the links provided in the manuscript.

Code availability Code is freely available from corresponding author upon request.

Declarations

Ethics approval We the undersigned declare that this manuscript is original, has not been published before, and is not under consideration for publication elsewhere.

Consent to participate Not applicable

Consent for publication All authors consented to publish the manuscript.

Conflict of interest The authors declare no competing interests.

References

- Abdi AM, Seaquist J, Tenenbaum DE, et al. (2014) The supply and demand of net primary production in the Sahel. *Environ Res Lett* 9. <https://doi.org/10.1088/1748-9326/9/9/094003>
- Adiguzel F, Bozdogan Sert E, Dinc Y, et al. (2021) Determining the relationships between climatic elements and thermal comfort and tourism activities using the tourism climate index for urban planning: a case study of Izmir Province: Tourism climate index for urban planning. *Theor Appl Climatol* 1–16. <https://doi.org/10.1007/s00704-021-03874-9>
- Ahmed M, Else B, Eklundh L et al (2017) Dynamic response of ndvi to soil moisture variations during different hydrological regimes in the sahel region. *Int J Remote Sens* 38:5408–5429. <https://doi.org/10.1080/01431161.2017.1339920>
- Aklesso M, Kumar KR, Bu L, Boiyo R (2018) Analysis of spatial-temporal heterogeneity in remotely sensed aerosol properties observed during 2005–2015 over three countries along the Gulf of

- Guinea Coast in Southern West Africa. *Atmos Environ* 182:313–324. <https://doi.org/10.1016/j.atmosenv.2018.03.062>
- Al-doski J, Mansor SB, Shafri HZM (2013) NDVI Differencing and post-classification to detect vegetation changes in Halabja City, Iraq. *J Appl Geol Geophys* 1:1–10
- Bachelet D, Neilson RP, Lenihan JM, Drapek RJ (2001) Climate change effects on ecosystem distribution and carbon budget in the United States. *Ecosystems* 4:164–185. <https://doi.org/10.1007/s10021-001-0002-7>
- Barbosa HA, Huete AR, Baethgen WE (2006) A 20-year study of NDVI variability over the Northeast Region of Brazil. *J Arid Environ* 67:288–307. <https://doi.org/10.1016/j.jaridenv.2006.02.022>
- Bégué A, Vintrou E, Ruelland D et al (2011) Can a 25-year trend in Soudano-Sahelian vegetation dynamics be interpreted in terms of land use change? A remote sensing approach. *Glob Environ Chang* 21:413–420. <https://doi.org/10.1016/j.gloenvcha.2011.02.002>
- Brandt M, Hiernaux P, Rasmussen K et al (2016) Assessing woody vegetation trends in Sahelian drylands using MODIS based seasonal metrics. *Remote Sens Environ* 183:215–225. <https://doi.org/10.1016/j.rse.2016.05.027>
- Brown J (2018) NDVI, The foundation for remote sensing phenology. In: usgs, Remote Sens. Phenol. [https://www.usgs.gov/special-topics/remote-sensing-phenology/science/ndvi-foundation-remote-sensing-phenology#:~:text=NDVIvaluesrangedfrom%2B1.0,\(approximately0.2to0.5\)](https://www.usgs.gov/special-topics/remote-sensing-phenology/science/ndvi-foundation-remote-sensing-phenology#:~:text=NDVIvaluesrangedfrom%2B1.0,(approximately0.2to0.5))
- Cetin M (2019) The effect of urban planning on urban formations determining bioclimatic comfort area's effect using satellitia imagines on air quality: a case study of Bursa city. *Air Qual Atmos Heal* 12:1237–1249. <https://doi.org/10.1007/s11869-019-00742-4>
- Cetin M (2020a) Peyzaj Planlama Aşamasında Önemli Etkilerden Olan Sıcaklık, Yağış Ve İklim Tiplerinde, Küresel İklim Değişikliğine Bağlı Olarak Meydana Gelebilecek Değişiklikler: Mersin Kent Örneği. *Turkish J Agric - Food Sci Technol* 8:2695–2701. <https://doi.org/10.24925/turjaf.v8i12.2695-2701.3891>
- Cetin M (2020b) Climate comfort depending on different altitudes and land use in the urban areas in Kahramanmaraş City. *Air Qual Atmos Heal* 13:991–999. <https://doi.org/10.1007/s11869-020-00858-y>
- Collins JM (2011) Temperature variability over Africa. *J Clim* 24:3649–3666. <https://doi.org/10.1175/2011JCLI3753.1>
- Dardel C, Kergoat L, Hiernaux P et al (2014) Re-greening Sahel: 30 years of remote sensing data and field observations (Mali, Niger). *Remote Sens Environ* 140:350–364. <https://doi.org/10.1016/j.rse.2013.09.011>
- Dool HVD (2003) Performance and analysis of the constructed analogue method applied to U.S. soil moisture over 1981–2001. *J Geophys Res* 108:1–16. <https://doi.org/10.1029/2002jd003114>
- Du J, Shu J, Yin J et al (2015) Analysis on spatio-temporal trends and drivers in vegetation growth during recent decades in Xinjiang, China. *Int J Appl Earth Obs Geoinf* 38:216–228. <https://doi.org/10.1016/j.jag.2015.01.006>
- Eklundh L, Olsson L (2003) Vegetation index trends for the African Sahel 1982–1999. *Geophys Res Lett* 30:1–4. <https://doi.org/10.1029/2002GL016772>
- Fensholt R, Proud SR (2012) Evaluation of Earth Observation based global long term vegetation trends - Comparing GIMMS and MODIS global NDVI time series. *Remote Sens Environ* 119:131–147. <https://doi.org/10.1016/j.rse.2011.12.015>
- Gilbert RO (1987) Statistical methods for environmental pollution monitoring. Wiley, New York
- Gu Z, Duan X, Shi Y, Li Y, Pan Xi (2018) Spatiotemporal variation in vegetation coverage and its response to climatic factors in the Red River Basin, China. *Ecological Indicators* 93:54–64. <https://doi.org/10.1016/j.ecolind.2018.04.033>
- Haglund E, Ndjeunga J, Snook L, Pasternak D (2011) Dry land tree management for improved household livelihoods: Farmer managed natural regeneration in Niger. *J Environ Manage* 92:1696–1705. <https://doi.org/10.1016/j.jenvman.2011.01.027>
- Hänke H, Börjeson L, Hylander K, Enfors-Kautsky E (2016) Drought tolerant species dominate as rainfall and tree cover returns in the West African Sahel. *Land Use Policy* 59:111–120. <https://doi.org/10.1016/j.landusepol.2016.08.023>
- Harris I, Jones PD, Osborn TJ, Lister DH (2014) Updated high-resolution grids of monthly climatic observations - the CRU TS3.10 Dataset. *Int J Climatol* 34:623–642. <https://doi.org/10.1002/joc.3711>
- Hashim H, Latif ZA, Adnan NA (2019) Urban vegetation classification with NDVI threshold value method with very high-resolution (VHR) pleiades imagery. pp 1–3
- Hein L, De RN, Hiernaux P et al (2011) Desertification in the Sahel: towards better accounting for ecosystem dynamics in the interpretation of remote sensing images. *J Arid Environ* 75:1164–1172. <https://doi.org/10.1016/j.jaridenv.2011.05.002>
- Herrmann S (2007) Variability of Sahelian rainfall and its impact on vegetation dynamics
- Herrmann SM, Anyamba A, Tucker CJ (2005) Recent trends in vegetation dynamics in the African Sahel and their relationship to climate. *Glob Environ Chang* 15:394–404. <https://doi.org/10.1016/j.gloenvcha.2005.08.004>
- Hoscilo A, Baltzer H, Bartholomé E et al (2015) A conceptual model for assessing rainfall and vegetation trends in sub-Saharan Africa from satellite data. *Int J Climatol* 35:3582–3592. <https://doi.org/10.1002/joc.4231>
- Igbawua T, Zhang J, Chang Q, Yao F (2016) Vegetation dynamics in relation with climate over Nigeria from 1982 to 2011. *Environ Earth Sci* 75. <https://doi.org/10.1007/s12665-015-5106-z>
- Jones PD, Hulme M (1996) Calculating regional climatic time series for temperature and precipitation: methods and illustrations. *Int J Climatol* 16:361–377. [https://doi.org/10.1002/\(SICI\)1097-0088\(199604\)16:4%3c361::AID-JOC53%3e3.0.CO;2-F](https://doi.org/10.1002/(SICI)1097-0088(199604)16:4%3c361::AID-JOC53%3e3.0.CO;2-F)
- Karlson M, Ostwald M (2016) Remote sensing of vegetation in the Sudano-Sahelian zone: a literature review from 1975 to 2014. *J Arid Environ* 124:257–269. <https://doi.org/10.1016/j.jaridenv.2015.08.022>
- Kaspersen PS, Fensholt R, Huber S (2011) A spatiotemporal analysis of climatic drivers for observed changes in Sahelian vegetation productivity (1982–2007). *Int J Geophys* 2011:1–20114. <https://doi.org/10.1155/2011/715321>
- Kendall MG (1975) Rank correlation methods., Griffin. London
- Kilicoglu C, Cetin M, Aricak B, Sevik H (2021) Integrating multicriteria decision-making analysis for a GIS-based settlement area in the district of Atakum, Samsun, Turkey. *Theor Appl Climatol* 143:379–388. <https://doi.org/10.1007/s00704-020-03439-2>
- Knauer K, Gessner U, Dech S, Kuenzer C (2014) Remote sensing of vegetation dynamics in West Africa. *Int J Remote Sens* 35:6357–6396. <https://doi.org/10.1080/01431161.2014.954062>
- Lambin EF, Ehrlich D (1997) Land-cover changes in Sub-Saharan Africa (1982–1991): application of a change index based on remotely sensed surface temperature and vegetation indices at a continental scale. *Remote Sens Environ* 61:181–200. [https://doi.org/10.1016/S0034-4257\(97\)00001-1](https://doi.org/10.1016/S0034-4257(97)00001-1)
- Leroux L, Bégué A, Lo Seen D et al (2017) Driving forces of recent vegetation changes in the Sahel: lessons learned from regional and local level analyses. *Remote Sens Environ* 191:38–54. <https://doi.org/10.1016/j.rse.2017.01.014>

- Li Z, Chen Y, Li W, et al. (2015) Journal of Geophysical Research : Atmospheres. 8817–8827. <https://doi.org/10.1002/2015JD023545>. Received
- Los SO (2013) Analysis of trends in fused AVHRR and MODIS NDVI data for 1982–2006: Indication for a CO₂ fertilization effect in global vegetation. *Global Biogeochem Cycles* 27:318–330. <https://doi.org/10.1002/gbc.20027>
- Lukamba M (2010) Natural disasters in African countries: what can we learn about them? *J Transdiscipl Res South Africa* 6:478–495
- Mann HB (1945) Non-parametric test against trend. *Econometrica* 13:245–259
- Martiny N, Philippon N, Richard Y, Camberlin P (2010) Predictability of NDVI in semi-arid African regions. 467–484. <https://doi.org/10.1007/s00704-009-0223-9>
- Müller C, Waha K, Bondeau A, Heinke J (2014) Hotspots of climate change impacts in sub-Saharan Africa and implications for adaptation and development. *Glob Chang Biol* 20:2505–2517. <https://doi.org/10.1111/gcb.12586>
- Mulugeta M, Tolossa D, Abebe G (2017) Description of long-term climate data in Eastern and Southeastern Ethiopia. *Data Br* 12:26–36. <https://doi.org/10.1016/j.dib.2017.03.025>
- Nath B, Acharjee S (2013) Forest cover change detection using normalized difference vegetation index (NDVI) : a study of Reinghyongkine lake's adjoining areas, Rangamati, Bangladesh. *Indian Cartogr XXXIII*:348–353
- Nicholson SE (1980) The nature of rainfall fluctuations in subtropical West Africa. *Mon Weather Rev* 108:473–487. [https://doi.org/10.1175/1520-0493\(1980\)108%3c0473:TNORFI%3e2.0.CO;2](https://doi.org/10.1175/1520-0493(1980)108%3c0473:TNORFI%3e2.0.CO;2)
- Nicholson SE (2000) The nature of rainfall variability over Africa on times scales of decades to millennia. *Glob Planet Change* 26:137–158
- Nicholson SE, Farrar TJ (1994) The influence of soil type on the relationships between NDVI, rainfall, and soil moisture in semiarid Botswana. I. NDVI response to rainfall. *Remote Sens Environ* 50:107–120. [https://doi.org/10.1016/0034-4257\(94\)90038-8](https://doi.org/10.1016/0034-4257(94)90038-8)
- Nicholson SE, Kim J (1997) the relationship of the El Niño–southern oscillation to African rainfall. *Int J Climatol* 17:117–135. [https://doi.org/10.1002/\(SICI\)1097-0088\(199702\)17:2%3c117::AID-JOC84%3e3.0.CO;2-O](https://doi.org/10.1002/(SICI)1097-0088(199702)17:2%3c117::AID-JOC84%3e3.0.CO;2-O)
- Ogou FK, Nduka V, Edward O, Chukwuemeka N (2021) Hydro-climatic and water availability changes and its relationship with NDVI in Northern Sub-Saharan Africa. *Earth Syst Environ*. <https://doi.org/10.1007/s41748-021-00260-3>
- Ogou FK, Yang Q, Duan Y, Ma ZZ-G (2019) Comparative analysis of interdecadal precipitation variability over central North China and sub Saharan Africa. *Atmos Ocean Sci Lett* 12:1–7. <https://doi.org/10.1080/16742834.2019.1593040>
- Okoro UK, Chen W, Chineke C, Nwofor O (2017) Anomalous atmospheric circulation associated with recent West African Monsoon Rainfall variability. *J Geosci Environ Prot* 1–27. <https://doi.org/10.4236/gep.2017.512001>
- Olsson L, Eklundh L, Ardö J (2005) A recent greening of the Sahel - trends, patterns and potential causes. *J Arid Environ* 63:556–566. <https://doi.org/10.1016/j.jaridenv.2005.03.008>
- Pei F, Wu C, Liu X et al (2018) Monitoring the vegetation activity in China using vegetation health indices. *Agric for Meteorol* 248:215–227. <https://doi.org/10.1016/j.agrformet.2017.10.001>
- Peng W, Kuang T, Tao S (2019) Quantifying influences of natural factors on vegetation NDVI changes based on geographical detector in Sichuan, western China. *J Clean Prod* 233:353–367. <https://doi.org/10.1016/j.jclepro.2019.05.355>
- Philippon N, Jarlan L, Martiny N et al (2007) Characterization of the interannual and intraseasonal variability of West African vegetation between 1982 and 2002 by means of NOAA AVHRR NDVI data. *J Clim* 20:1202–1218. <https://doi.org/10.1175/JCLI4067.1>
- Pinzon JE, Brown ME, Tucker CJ (2005) Hilbert-Huang transform and its applications., N.E. Huang. Singapore; Hackensack, NJ; London: World Scientific
- Pinzon JE, Tucker CJ (2014) A non-stationary 1981–2012 AVHRR NDVI3g time series. *Remote Sens* 6:6929–6960. <https://doi.org/10.3390/rs6086929>
- Pravalié R, Sîrodoev I, Peptenatu D (2014) Detecting climate change effects on forest ecosystems in Southwestern Romania using Landsat TM NDVI data. *J Geogr Sci* 24:815–832. <https://doi.org/10.1007/s11442-014-1122-2>
- Rishmawi K, Prince SD, Xue Y (2016) Vegetation responses to climate variability in the Northern arid to sub-humid zones of Sub-Saharan Africa. <https://doi.org/10.3390/rs8110910>
- Sasson I, Weinreb A (2017) Land cover change and fertility in West-Central Africa: rural livelihoods and the vicious circle model. *Popul Environ* 38:345–368. <https://doi.org/10.1007/s11111-017-0279-x>
- Schlenker W, Lobell DB (2010) Robust negative impacts of climate change on African agriculture. *Environ Res Lett* 5. <https://doi.org/10.1088/1748-9326/5/1/014010>
- Sindikubwabo C, Li R, Wang C (2018) Abrupt change in Sahara precipitation and the associated circulation patterns. *Atmos Clim Sci* 08:262–273. <https://doi.org/10.4236/acs.2018.82017>
- Spiekermann R, Brandt M, Samimi C (2015) Woody vegetation and land cover changes in the Sahel of Mali (1967–2011). *Int J Appl Earth Obs Geoinf* 34:113–121. <https://doi.org/10.1016/j.jag.2014.08.007>
- Swaine MD (1992) Characteristics of dry forest in West Africa and the influence of fire. *J Veg Sci* 3:365–374
- Traore SB, Ali A, Tinni SH et al (2014) AGRHYMET: a drought monitoring and capacity building center in the West Africa Region. *Weather Clim Extrem* 3:22–30. <https://doi.org/10.1016/j.wace.2014.03.008>
- Tucker CI (1986) Maximum normalized difference vegetation index images for subSaharan Africa for 1983–1985. *Int J Remoyte Sens* 7:1383–1384
- Vlek P, Le QB, Tamene L (2008) Land decline in Land-Rich Africa—a creeping disaster in the making. Italy, Rome
- Wagner RG, da Silva AM (1994) Surface conditions associated with anomalous rainfall in the guinea coastal region. *Int J Climatol* 14:179–199. <https://doi.org/10.1002/joc.3370140205>
- Wang J, Rich PM, Price KP (2003) Temporal responses of NDVI to precipitation and temperature in the Central Great Plains, USA. *Int J Remote Sens* 24:2345–2364. <https://doi.org/10.1080/0143160210154812>
- Xu G, Zhang H, Chen B, et al. (2014) Changes in vegetation growth dynamics and relations with climate over China's landmass from 1982 to 2011. 3263–3283. <https://doi.org/10.3390/rs6043263>
- Xu HJ, Wang XP, Zhang XX (2016a) Decreased vegetation growth in response to summer drought in Central Asia from 2000 to 2012. *Int J Appl Earth Obs Geoinf* 52:390–402. <https://doi.org/10.1016/j.jag.2016.07.010>
- Xu Y, Yang J, Chen Y (2016b) NDVI-based vegetation responses to climate change in an arid area of China. *Theor Appl Climatol* 126:213–222. <https://doi.org/10.1007/s00704-015-1572-1>
- Yang Y, Wang S, Bai X et al (2019) Factors affecting long-term trends in global NDVI. *Forests* 10:1–17. <https://doi.org/10.3390/f10050372>

- Yim S, Bin W, Jian L, Zhiwei W (2014) A comparison of regional monsoon variability using monsoon indices. *Clim Dyn* 43:1423–1437. <https://doi.org/10.1007/s00382-013-1956-9>
- Zewdie W, Csaplovics E, Inostroza L (2017) Monitoring ecosystem dynamics in northwestern Ethiopia using NDVI and climate variables to assess long term trends in dryland vegetation variability. *Appl Geogr* 79:167–178. <https://doi.org/10.1016/j.apgeog.2016.12.019>
- Zhang H, Chang J, Zhang L et al (2018) NDVI dynamic changes and their relationship with meteorological factors and soil moisture. *Environ Earth Sci* 77:1–11. <https://doi.org/10.1007/s12665-018-7759-x>
- Zhang X, Friedl MA, Schaaf CB et al (2005) Monitoring the response of vegetation phenology to precipitation in Africa by coupling MODIS and TRMM instruments. *J Geophys Res D Atmos* 110:1–14. <https://doi.org/10.1029/2004JD005263>
- Zhang X, Wu S, Yan X, Chen Z (2017) A global classification of vegetation based on NDVI, rainfall and temperature. *Int J Climatol* 37:2318–2324. <https://doi.org/10.1002/joc.4847>
- Zhang Y, Zhang C, Wang Z et al (2016) Vegetation dynamics and its driving forces from climate change and human activities in the Three-River Source Region, China from 1982 to 2012. *Sci Total Environ* 563–564:210–220. <https://doi.org/10.1016/j.scitotenv.2016.03.223>

Publisher's note Springer Nature remains neutral with regard to jurisdictional claims in published maps and institutional affiliations.